

# Interaction of Acoustic Waves with Cracks: Elastic and Inelastic Nonlinearity Mechanisms on Different Time Scales

V. Yu. Zaitsev\*, V. É. Gusev\*\*, V. E. Nazarov\*, and B. Castagnède\*\*

\* *Institute of Applied Physics, Russian Academy of Sciences,  
ul. Ul'yanova 46, Nizhni Novgorod, 603950 Russia  
e-mail: vyuzai@hydro.appl.sci-nnov.ru*

\*\* *Université du Maine, Av. O. Messiaen, 72 085 Le Mans, France*

Received May 24, 2004

**Abstract**—The interrelated elastic and inelastic fast and slow effects of acoustic wave interaction with cracks are discussed from a unified point of view. Special attention is given to the dissipative manifestations of the presence of cracks and to the effects of the symmetrically time-reversible slow dynamics observed for acoustically activated cracks. These effects can be more pronounced than the conventionally discussed nonlinear elastic effects (such as higher harmonic generation). Taking into account the main geometric features of cracks, a thermoelastic mechanism is proposed to consistently interpret the experimental data. Consequences of the results of these studies for seismics are discussed, and the possibilities of using the observed effects for nonlinear acoustic diagnostics of cracks are discussed. © 2005 Pleiades Publishing, Inc.

## INTRODUCTION

Today, it is generally recognized that the presence of cracks causes considerable changes in the linear and nonlinear acoustic properties of solids (as compared to perfect crystals and homogeneous amorphous materials). In particular, one should note the high level of acoustic nonlinearity and its nonclassical character (e.g., nonmonotonic and fractional-power amplitude dependences for the harmonics of the signal), an enhanced absorption of elastic waves, the dependence of dissipation on the wave amplitude and on the static pressure on the sample, and pronounced effects of slow dynamics (the memory for the preliminary acoustic activation and the logarithmic behavior in time). When the concentration of cracks is relatively high, the linear elastic moduli of the material may also be noticeably reduced, but, in the case of a low defect concentration, the elasticity of the material remains almost the same while the absorption and the nonlinear properties may already be noticeably changed.

Evidently, all these manifestations are associated with the relative “softness” of cracks, although some of the conventional reasoning leaves a number of significant questions open to discussion. The popular radio engineering analogy is based on the statement that cracks can be considered as diode-like elements: under tensile stress, they are easily opened, and under compression stress, they are closed, so that, under compression, the material behaves as an intact solid. For sufficiently large strains, this interpretation of the nonlinearity of cracks may be useful, but the question of how the cracks can considerably change their state under mod-

erate strains on the order of  $10^{-6}$  or less remains open, because, at such strains, the acoustic nonlinearity of the material usually becomes noticeable. Many of the defect models predict [1] that a crack can be almost completely closed when the mean compression strain in the material is approximately equal to the crack's aspect ratio  $d/L$ , where  $d$  and  $L$  are the characteristic values of the opening (thickness) and the diameter of the crack, respectively. Typical values of this ratio for cracks, e.g., in rock, are within  $10^{-4}$ – $10^{-3}$ . For the acoustic parameters (such as absorption or elastic moduli) of cracked media, this leads to their pronounced dependence on the applied pressure until the mean strain of the material reaches  $10^{-4}$ – $10^{-3}$ . Then, the pressure-dependent parameters flatten out approaching the values typical of the homogeneous material, which testifies that the cracks are completely closed (see, e.g., [2]). An acoustic action on the material with moderate mean strains  $\varepsilon \sim 10^{-6}$ – $10^{-5}$  also leads to noticeable changes in the time-average elasticity and dissipation (which can be observed by the changes in the parameters of the resonance peaks of a weaker probing wave, as described in, e.g., [3]). If we assume that the change in the properties of the material in the presence of such small strains is associated with the closure of the narrowest cracks with the aspect ratio  $d/L \sim 10^{-6}$  or smaller, we obtain that, for the millimeter or submillimeter cracks, which are typical of rock, their average opening  $d$  is about the atomic size or smaller. This conclusion is physically meaningless and points to the necessity to improve the aforementioned radio engineering analogy.

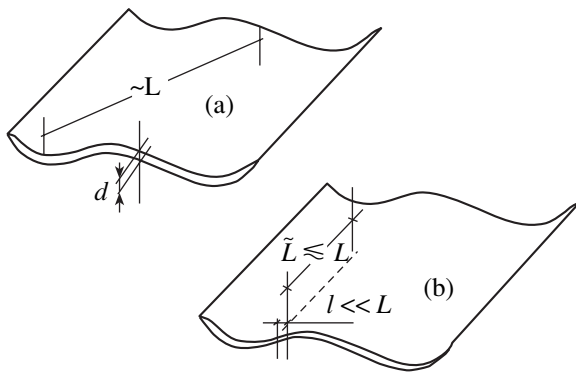


**Fig. 1.** Crack with wavy surfaces (a) without an internal contact and (b) with an internal contact with the dimensions  $\tilde{L} \times l$ . When  $\tilde{L} \rightarrow l$ , the line contact transforms to a point contact.

We note that, in view of the enhanced dissipation of elastic waves in cracked media, models that ascribe this loss to the friction and/or adhesion hysteresis at the crack surfaces were developed within the last 40 years (see, e.g., [4, 5]). Such models give reasonable estimates of losses for waves of sufficiently large amplitudes, including the prediction of an almost constant  $Q$  factor of a material in a wide frequency range. However, in the framework of these models, no explanation can be found for the low-amplitude (linear) absorption. The following citation from [4] clarifies the problem: "...For the range of strains used in our experiments, an upper limit of interface displacement [at a crack surface] ranges from  $10^{-12}$  cm in the low strain amplitude experiments... The displacements are so small [3–4 orders of magnitude smaller than the atomic size] that the friction characteristics of the interfaces should be quite different from what would be observed in a macroscopic friction experiment..." The atomic-force microscopy data obtained in recent years demonstrate the threshold character of the friction-hysteresis loss, whose manifestation requires that the absolute displacement at the contacting surfaces exceeds the atomic size (see, e.g., [6]). On the other hand, the loss observed in the experiment is much greater than that in homogeneous materials even for ultimately small wave amplitudes, which points to the presence of a nonthreshold mechanism of elastic energy dissipation by the cracks.

One version of such a nonthreshold thermoelastic mechanism of loss in solid bodies with cracks was proposed by Savage [7]. Unlike the insignificant role of such a loss in a homogeneous solid, the presence of cracks strongly increases the loss owing to the introduction of the additional scale characterizing the inhomogeneity of thermoelastic fields and being much smaller than the elastic wavelength. The frequency dependence of this loss has a maximum which corresponds to the coincidence of the thermal wavelength with the characteristic diameter of a crack. The analysis

performed in [7] shows that such a mechanism predicts reasonable values for the elastic wave dissipation in the seismic frequency range. Assuming a wide distribution of cracks in size, in this model it is also possible to obtain an almost constant value of the  $Q$  factor in a broad frequency range. However, since, in the framework of this mechanism, the maximum energy loss rapidly decreases with decreasing diameter of the crack (as the inverse cube of the diameter), the approximately constant  $Q$  factor of rock observed in the frequency range from hertz to megahertz can be explained only by assuming the presence of unreasonably high concentrations of extremely small cracks. In addition, to explain the pronounced amplitude dependence of absorption in cracked media for moderate strain amplitudes  $\varepsilon \sim 10^{-6}$ , the thermoelastic mechanism [7] requires the assumption that high concentrations of cracks with unlikely small aspect ratio  $d/L$  are present.

In this paper, we discuss the mechanism of acoustic nonlinearity of cracks that eliminates the aforementioned discrepancies and allows us from a unified point of view not only to consider the linear (small-amplitude) absorption and its fast amplitude-dependent variations but also to take into account the effects of slow dynamics. In addition, we present the results of experiments on the nonlinear interaction of acoustic waves with cracks in rods and plates. These results agree well with the proposed interpretation.

#### BASIC GEOMETRIC FEATURES OF CRACKS AND THEIR PHYSICAL CONSEQUENCES

As was noted above, a crack is a planar defect of a solid with a small aspect ratio  $d/L \ll 1$  (its typical values are  $d/L \sim 10^{-4} - 10^{-3}$ ). Hence, for a complete closure of a crack, it is necessary to produce a mean strain in the material on the order of  $d/L$ . This estimate weakly depends on the details of the crack model [1] and proves to be much greater than the typical acoustic wave amplitudes  $\varepsilon \sim 10^{-6} - 10^{-5}$  at which the aforementioned nonlinear elastic and dissipative effects become noticeable. Another important feature of cracks, which follows from their images obtained with optical, electron, and atomic-force microscopies and agrees well with the known models of crack formation, is that the contacting surfaces of cracks are usually wavy rather than flat (i.e., their shape resembles a series of ridges and valleys rather than a set of local peaks and dips). When the crack is formed, these initially matched wavy surfaces not only move in different directions along the normal but also are shifted in the tangential direction forming internal contacts. Because of the wavy curvature of the crack surfaces, the resulting contacts are not of a point character but are extended in one direction, as shown in Fig. 1 [8]. It is essential that, in the vicinity of a contact, the local distance between the crack surfaces (or their mutual penetration)  $\tilde{d}$  is much smaller than the

average distance  $d$  of the crack opening. Owing to this geometry, the vicinity of the contact is more sensitive to external stress (by a factor of about  $d/\tilde{d} \gg 1$ ) than the crack as a whole. Therefore, the state of the contacts in a crack may considerably change in the presence of a relatively weak mean strain in the medium:  $\varepsilon \sim 10^{-6}$ – $10^{-5}$  (which is much smaller than the strain  $\varepsilon \sim d/L \sim 10^{-4}$ ... $10^{-5}$  necessary for a complete closure of the crack).

In connection with this, a question arises as to whether these contacts, which are very small compared to the whole crack, are capable of absorbing a considerable amount of acoustic energy. For the manifestation of the commonly discussed friction and adhesion losses at the contacts, it is necessary (as was noted above) that the displacements of the surfaces in the contact region be greater than the atomic size  $a$ . For a crack with a characteristic diameter  $L$ , the mean strain  $\varepsilon$  (be it compression or tension) produced in the medium may cause a maximum displacement of the contacting surfaces of the crack (in either the tangential or the normal direction) on the order of  $\Delta \sim \varepsilon L$  [8–10]. As noted in [9], this estimate does not depend on the details of the crack model and agrees well with the above statement that an mean compression strain of about the aspect ratio of the crack,  $\Delta \sim d/L$ , causes the displacement of contacting surfaces  $\Delta \approx d$ , which results in a complete closure of the crack. On the other hand, the condition that  $\Delta$  exceeds the atomic size  $a$  ( $\Delta > a$ ) determines the threshold mean strain  $\varepsilon_{th} > a/L$ , below which the displacement of the surfaces occurs on a subatomic scale. For the typical value  $a \sim 3 \times 10^{-10}$  m and crack size  $L \sim 10^{-3}$  m, the threshold mean strain is  $\varepsilon_{th} \sim 3 \times 10^{-7}$  (which agrees well with the threshold of the amplitude-dependent loss observed experimentally). Below this value, the adhesion and friction losses on the crack surface cannot be activated.

At the same time, even for a much smaller strain, a channel for a rather effective dissipation of the acoustic wave energy is formed owing to the locally enhanced thermoelastic loss. This possibility was demonstrated in [7] with the use of the exact solution obtained for an elliptic crack. Indeed, in the presence of stress and strain inhomogeneities (due to the microstructure of the material), the gradients of temperature variations induced by an elastic disturbance are determined not by the elastic wavelength but by the much smaller inhomogeneity scale  $L$  or by the thermal wavelength  $\delta$  itself [11]. When the crack size  $L$  and  $\delta$  coincide, the elastic energy loss at the crack as a whole is maximum [7]. A similar result can be obtained without specifying the crack model in detail, by estimating the temperature gradients and the corresponding losses in the vicinity of the crack on the basis of the approach used in [11] in application to losses in polycrystals. When applied to a crack, this approach yields the following approximate

expressions for the elastic energy loss  $W$  per period for the low-frequency limit ( $L \ll \delta$ ), the high-frequency limit ( $L \gg \delta$ ), and the vicinity of the relaxation maximum ( $L \sim \delta$ ) [8]:

$$W_{LF} \approx 2\pi\omega T(\alpha^2 K^2/\kappa)L^5\varepsilon^2, \quad \omega \ll \omega_L \approx \kappa/(\rho CL^2), \quad (1)$$

$$W_{HF} \approx 2\pi T(\alpha^2 K^2/\rho C)[\kappa/(\rho C\omega)]^{1/2}L^2\varepsilon^2, \quad \omega \gg \omega_L, \quad (2)$$

$$W_{crack}^{max} \approx 2\pi T(\alpha^2 K^2/\rho C)L^3\varepsilon^2, \quad \omega \approx \omega_L, \quad (3)$$

where  $\omega$  is the circular frequency,  $T$  is the temperature,  $\alpha$  is the coefficient of volumetric thermal expansion,  $K$  is the bulk modulus,  $\rho$  is the density,  $C$  is the specific heat,  $\varepsilon$  is the mean strain in the medium,  $\kappa$  is the thermal conductivity coefficient, and  $\omega_L$  is the characteristic thermal relaxation frequency corresponding to the size  $L$  of the crack. For example, for  $L \sim 1$  mm, the relaxation frequency  $\omega_L$  falls within  $(10^{-1}-1)$  rad/s for most types of rock and metals. In determining the low-frequency loss (1), by analogy with [11], we took into account that the crack size  $L$  is the characteristic scale within which the elastic stress changes from the mean value  $\sigma$  to zero at the free boundaries of the crack. In deriving the high-frequency asymptotics (2), we used the fact that different crack models identically predict a tip stress concentration of the form  $\sigma_{tip} \sim \sigma/\sqrt{r/L}$  [12] (where the distance  $r$  is measured with respect to the crack tip). Precisely this region gives the main contribution to the high-frequency dissipation. Expression (3) for estimating the maximum loss is obtained from the condition of equality of the low- and high-frequency asymptotics, which is achieved when the characteristic thermal wavelength coincides with the size of the defect. Solutions (1)–(3), being independent of the details of the crack model, agree well with the exact solution [7] obtained for elliptic cracks.

To obtain similar estimates of the thermoelastic loss at the internal contact, it is necessary to take into account the stress distribution between the contact itself and the arc stiffness of the crack as a whole. For the contacts, which are soft compared to the crack rigidity, this leads to the situation where the stress  $\sigma_c$  at the contact exceeds the mean stress  $\sigma$  by a factor of about  $L/l \gg 1$ ; i.e.,  $\sigma_c \sim \sigma(L/l)$  (but not proportional to  $(L/l)^2$ , as assumed in, e.g., [5]). The region of the near-contact stress localization penetrates into the material to a depth of about the contact width  $l \ll L$  [13]. (We note that the aforementioned features of the stress distribution do not depend on the details of the crack and contact models.) Then, the application of the approach used in [11] leads to the following expressions for the

thermoelastic energy loss per period at a contact of length  $\tilde{L}$  and width  $l$ :

$$W_{LF} \approx 2\pi\omega T(\alpha^2 K^2/\kappa)l^2\tilde{L}L^2\varepsilon^2, \quad (4)$$

$$\omega \ll \omega_l \approx \kappa/(\rho Cl^2),$$

$$W_{HF} \approx (2\pi/\omega)\kappa T(\alpha K/C\rho)^2\tilde{L}(L/l)^2\varepsilon^2, \quad \omega \gg \omega_l, \quad (5)$$

$$W_{\text{cont}}^{\text{max}} \approx 2\pi T(\alpha^2 K^2/\rho C)\tilde{L}L^2\varepsilon^2, \quad \omega \approx \omega_l. \quad (6)$$

Structurally, these expressions resemble Eqs. (1)–(3), although the high-frequency asymptotics of the contact loss is  $\sim\omega^{-1}$ , which differs from  $\omega^{-1/2}$  obtained for narrow cracks. This is caused by the difference in the characters of stress concentration at the contact and at the crack perimeter, near which the high-frequency loss at the crack as a whole is localized: the latter is described by Eq. (2) obtained under the condition  $\delta \ll L$ . The comparison of Eqs. (3) and (6) for the loss in the vicinity of the relaxation maximum leads to a result that is unexpected at a first glance: for contacts with the length  $\tilde{L} \sim L$ , the maximum loss at the crack as a hole and at a narrow contact with a much smaller area prove to be on the same order of magnitude, although the relaxation maximum for the narrow contact  $l \ll L$  may lie at a point whose coordinate on the frequency axis is 4–6 orders of magnitude greater and fall in the kilohertz or even megahertz frequency range. Expressions (1)–(6) for losses per period at a single crack or at a contact make it possible, for a given defect concentration, to estimate the damping decrement in the medium by the known relation  $\theta = W/(2W_{\text{elast}})$ , where  $W_{\text{elast}}$  is the elastic energy in the wave per unit volume of the material and  $W$  is the energy loss per period in the same volume.

#### *Consequences for the Small-Amplitude Absorption*

The expressions presented above point to the necessity to reconsider the popular assumption that the thermoelastic loss is insignificant for, e.g., seismic waves. For small-amplitude waves ( $\varepsilon \leq 10^{-7}$ – $10^{-9}$ ), the aforementioned thermoelastic loss mechanism may even predominate. From Eqs. (1)–(6), it follows that cracks with several soft contacts may cause a noticeable thermoelastic absorption in a frequency range extending over several orders of magnitude (from the relaxation frequency of the crack to the relaxation frequencies of the contacts). Consider a crack of size  $L$  containing a single contact of width  $l \ll L$  and length  $\tilde{L} \sim L$ . This contact, in the vicinity of its relaxation frequency  $\omega_l$ , causes a dissipation that is approximately equal to the dissipation caused by  $N = (L/l)^3 \gg 1$  microcracks of size  $l$  with the same relaxation frequency [7]. The equivalent number of microcracks  $N$  may be great: for the typical ratio  $L/l \sim 10^2$  observed for real cracks, this number is  $N \sim 10^6$ . In view of the wide distribution in size of

cracks in real rocks, for realistic crack concentrations, the aforementioned mechanism predicts a weakly varying damping decrement in a wide frequency range, from fractions of hertz to ultrasonic frequencies. This result agrees with [7], but it was obtained without assuming unreasonably high concentrations of microcracks to account for the high-frequency loss.

#### *The Possibility of Observing Nonlinear Effects at Moderate Amplitudes*

Another important consequence of the above consideration is the conclusion that moderate mean strains  $\varepsilon \sim 10^{-6}$ – $10^{-5}$ , which often are too small to cause any noticeable changes in the state of the crack as a whole, can considerably change the dimensions  $l$  and  $\tilde{L}$  of individual contacts between the crack surfaces. According to Eqs. (4)–(6), these changes may noticeably affect the dissipation of a weak probing wave (even if the adhesion-hysteresis and friction losses remain insignificant for this wave). Specifically, this mechanism (possibly, along with other mechanisms of amplitude-dependent dissipation) predicts that, in cracked media, favorable conditions may be formed for the acoustic analog of the Luxembourg–Gorki effect, which was one of the first manifestations of the nonlinear interaction of waves observed experimentally [14]. The effect consists in the amplitude modulation transfer from one intense radio wave to another harmonic wave as a result of their interaction in the ionospheric plasma (this effect was first detected in 1933 for the radiation of high-power radio stations in Luxembourg and in Gorki). In this effect, the presence of components with frequencies  $\omega_1 \pm \Omega$  in the spectrum of the modulated intense wave leads to the appearance of modulation components with frequencies  $\omega_2 \pm n\Omega$  ( $n = 1, 2, \dots$ ) in the initially harmonic wave of frequency  $\omega_2$ . Such a cross-modulation is caused by the changes induced at low frequencies  $n\Omega$  in the absorption of the probing wave (because of the nonlinearity of the plasma). Small variations in the propagation velocity were insignificant for this effect [15]. (A similar effect of sound-by-sound amplitude modulation was observed in a field experiment for the interaction of seismoacoustic waves in a sandy ground with a dissipative acoustic nonlinearity [16].) Below, we present the results of observation of the elastic wave interaction in samples with single cracks, including the cross-modulation of the Luxembourg–Gorki type and the effects of the “slow dynamics” of acoustically activated cracks, for which the aforementioned features of cracks and contacts play an important role.

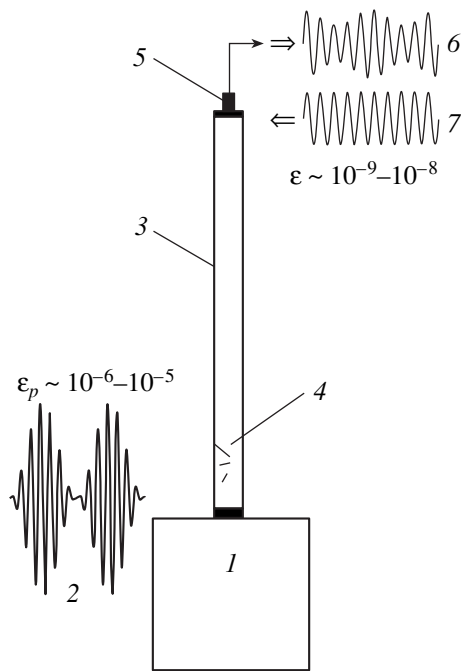


**Fig. 2.** Schematic diagram of the experiment: (1) loading mass with a piezoelectric transducer, (2) modulated pumping with  $\varepsilon_p \sim 10^{-6}$ – $10^{-5}$ , (3) a glass rod 8 mm in diameter and 30 cm in length, (4) cracks made by a thermal shock, (5) accelerometer and the source of the probing wave with  $\varepsilon \sim 10^{-9}$ – $10^{-8}$ , (6) the shape of the nonmodulated transmitted probing signal, and (7) the shape of the modulated received probing signal.

## EXPERIMENTAL RESULTS AND THEIR INTERPRETATION

### *Observation of the Analog of the Luxembourg–Gorki Cross-Modulation for Elastic Waves at Cracks*

The experiments (including the acoustic analogue of the Luxembourg–Gorki effect [8, 17]) were performed with the interaction of longitudinal resonance modes in glass rods (8 mm in diameter and 25–30 cm in length) containing one to three thermally initiated curved cracks with a size  $L$  of about 2–4 mm. The schematic diagram of an experiment is shown in Fig. 2. In these experiments, the amplitudes and frequencies of acoustic waves were measured with accuracies of  $\pm 0.01$  dB and  $\pm 0.5$  Hz, respectively. Figure 3a shows an induced modulation spectrum observed for the probing wave with the amplitude  $\varepsilon \sim 10^{-8}$  under the effect of an intense pumping wave that was amplitude-modulated with a frequency of several hertz. In the reference sample without cracks, the level of the modulation components (because of the background nonlinearity of the material and the equipment) was 25–40 dB lower than that in the sample with cracks. The resonance curves obtained for the probing wave with different levels of intense sinusoidal pumping at another mode (Fig. 3b) clearly demonstrate that the pumping primarily affects

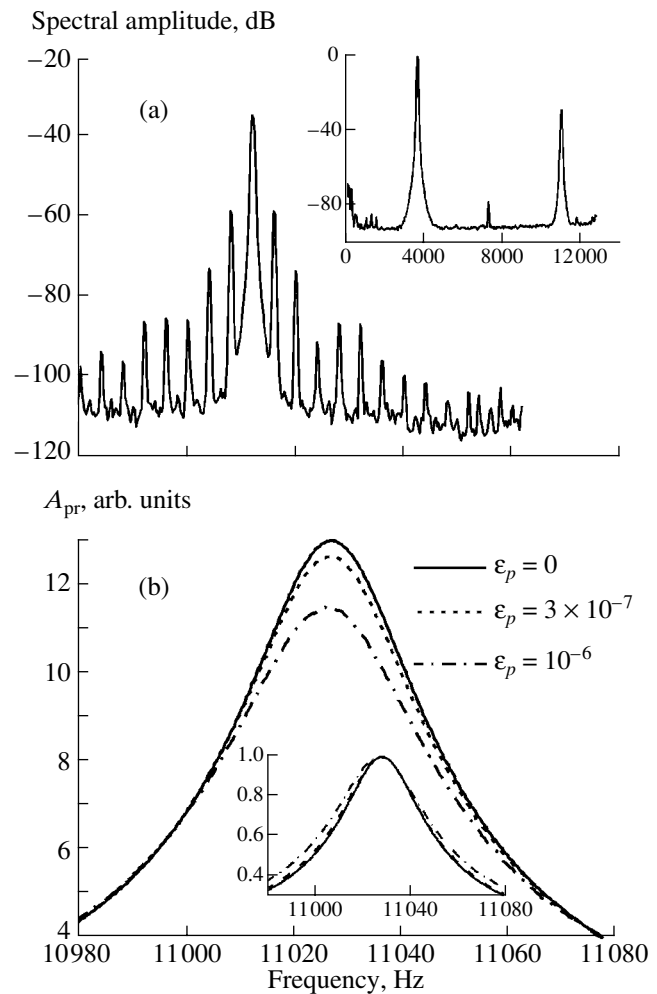


**Fig. 3.** Experimental observation of the Luxembourg–Gorki effect for acoustic waves. (a) Modulation spectrum of the probing wave at the second mode of the resonator ( $F = 11$  kHz) with the amplitude  $\varepsilon \sim 10^{-8}$  under the effect of the 3-Hz-modulated intense ( $\varepsilon_p \sim 10^{-6}$ ) pumping at the first mode ( $F = 3.6$  kHz); the inset shows the relative levels of the pumping and probing waves. (b) Resonance curves of the probing wave for different levels of the pumping wave; the curves demonstrate more than 10% variations of the  $Q$  factor for the probing mode in contrast to the virtually invariable resonance frequency; the inset shows the same curves in the normalized form.

the  $Q$  factor of the resonance while the change in its position plays a secondary role. The damping decrement of the probing wave and the levels of the modulation components depend (nonmonotonically in many cases [17]) on the pumping amplitude, but, with respect to the amplitude of the weak probing wave, these levels are linear. Quantitative estimates by Eqs. (4)–(6) for two or three cracks of millimeter size with internal line contacts show that, for the probing wave, this mechanism may cause a change of about 10% in the  $Q$  factor of the sample under study (with the initial value  $Q \sim 300$ – $350$ ) as a result of “turning on and off” the contacts

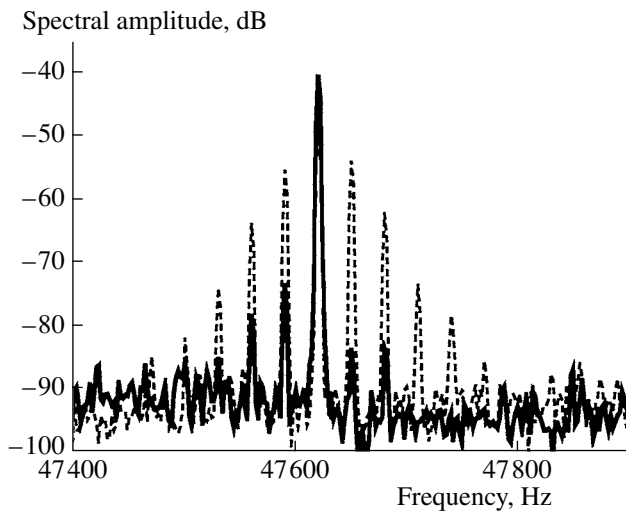


**Fig. 4.** Example of the Luxembour–Gorki cross-modulation in a glass plate with an artificial cracklike defect in the form of a cut with an inserted plate (the dashed line refers to the cut with the inserted plate, and the solid line, to the cut without the plate).

by the pumping wave. The decisive role of the crack for this effect was demonstrated by independent experiments with a glass plate that had a cut into which a metal plate could be inserted (and then eliminated) to form an artificial cracklike defect (Fig. 4). The results of this reference experiment correlate with the results of other experiments with real cracks, because they show that, for the effects under investigation, the contribution of the possible manifestations of nonlinearity at the points where radiators and receivers are attached to the sample (as well as the nonlinearity of the transducers themselves) is insignificant. Indeed, in the comparison of samples with real cracks and without them, the attachment areas inevitably were different and, in principle, they could be responsible for the difference in the results. In the experiment with the artificial defect (controlled by the plate inserted into the cut), the sample under study, together with the radiators and the receiver, was the same and, hence, the observed nonlinear effects were definitely associated with the manifestation of the nonlinearity of the cracklike defect.

#### *Induced Transparency and Induced Dissipation*

To understand the following experimental results [18] obtained for resonators of the aforementioned type, it is necessary to remember that the frequency corresponding to the maximum thermoelastic absorption,  $\omega = \omega_l \approx D/l^2$  ( $D = \kappa/\rho c$  is the thermal diffusivity), at the internal contact of the crack is determined by the contact width  $l$ , and that, when  $l$  is on the order of one or several microns, this frequency estimated for glass falls into the kilohertz frequency range. As was noted

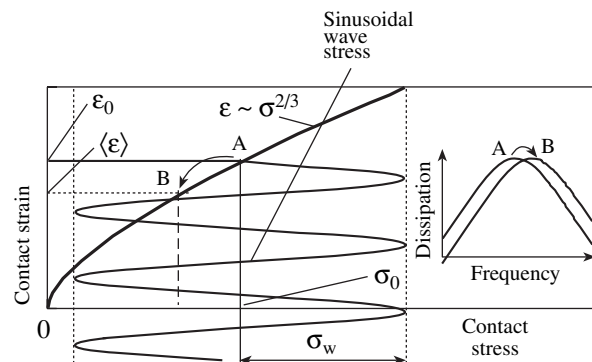


**Fig. 5.** Schematic representation of the softening of a Hertzian contact by an oscillating action because of the asymmetric dependence of its compression on the applied elastic stress. The unperturbed static equilibrium position  $A = (\sigma_0, \epsilon_0)$  and the shifted position  $B = (\langle \sigma \rangle, \langle \epsilon \rangle)$ . In the case of the contact between the surface reliefs in the form of hemispheres of radius  $R$  that move a distance of  $2\Delta$  closer to each other under the action of a force  $F$ , the compression strain is  $\epsilon_0 = \Delta/R$  and  $\sigma_0 = F/R^2$ , where these quantities are much smaller than the local strain and stress at the point of contact.

above, a moderate mean strain  $\epsilon \sim 10^{-6}$ – $10^{-5}$  can considerably change the width of the contact in the crack, which is also true when the action is of an oscillating character. For example, for a contact with the equilibrium compression strain  $\epsilon_0$  under the effect of the stress  $\sigma_0$ , where these quantities are related by the Hertz law  $\epsilon_0 \sim \sigma_0^{2/3}$  [11], an oscillating stress  $\sigma_w$ , comparable to  $\sigma_0$  may considerably reduce the mean compression of the contact  $\langle \epsilon \rangle$ , as schematically illustrated in Fig. 5. It should be noted that such a demodulation (rectification of oscillations) had been observed for both the macroscopic contact nonlinearity of contacting surfaces [19] and the so-called ultrasonic mode of atomic-force microscopy [20]. A consequence of such an average decrease in the contact width should be a shift of the relaxation maximum  $\omega_l$  of thermoelastic loss toward higher frequencies (see the inset in Fig. 4). As a result of this upward shift of  $\omega_l$ , the  $Q$  factor of the resonator for oscillations with frequencies below  $\omega_l$  should increase while, for higher frequency modes, to which the relaxation maximum has become closer, the  $Q$  factor may decrease. Among several samples with cracks (the parameters of contacts in the cracks were for the most part random), we succeeded in finding a sample that clearly demonstrated the aforementioned behavior. From Fig. 6, one can see that, in this sample, at the first longitudinal resonance lying below 4 kHz, the  $Q$  factor increased (from  $98 \pm 1$  to  $117 \pm 1$ ) under the effect of the pumping field whose frequency was an order of magnitude higher, whereas at the next resonance observed at about 10 kHz (as well as at other higher frequency resonances), the  $Q$  factor simultaneously



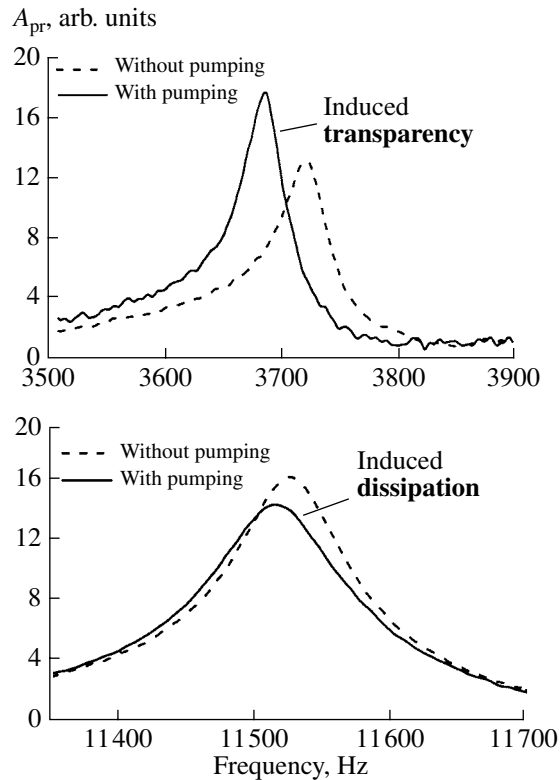


**Fig. 6.** Resonance curves of the probing wave simultaneously measured at different modes under the effect of pumping. The mode at the frequency  $F = 3.7$  kHz exhibits a dissipation decrease, whereas, for the mode with  $F = 11.5$  kHz, the loss increases. Unlike the opposite changes in losses, the frequencies of both modes are shifted downward. The pumping level (at  $F = 40\text{--}50$  kHz) is  $\varepsilon \sim 10^{-6}$ .

decreased (from  $154 \pm 1$  to  $115 \pm 1$ ). In contrast to the aforementioned opposite changes in the  $Q$  factors, the resonance frequencies of all observed peaks were simultaneously shifted downward, as one would expect because of the “softening” of the contact with an average decrease in its width.

A further increase in the wave amplitude  $\sigma_w > \sigma_0$  should switch the contact to the clapping regime. For this case, the Hertz law predicts that the average rigidity, as well as the contact width, should again increase. Then, one should expect a nonmonotonic behavior of the parameters of the probing resonance with increasing pumping amplitude: a tendency for an increase in the resonance frequency and an increase in the  $Q$  factor of the resonance after its decrease at smaller pumping amplitudes. All these features were also observed in the experiment, which can be seen in Fig. 7. The inset in Fig. 7 represents the calculated (by the Hertz model) variation of the period-average compression of the contact  $\langle \varepsilon \rangle$  as a function of the oscillating stress amplitude  $\sigma_w$ , normalized to the static stress  $\sigma_0$ .

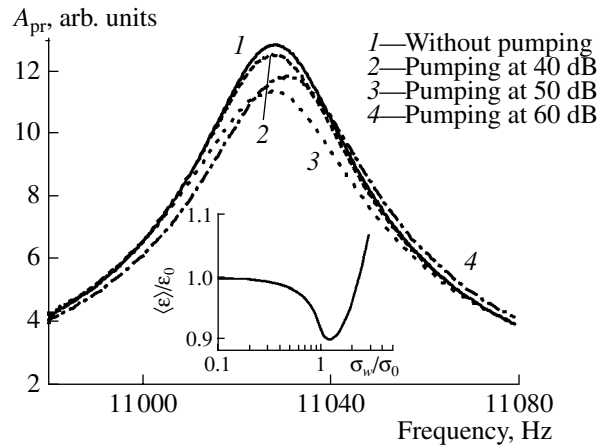


**Fig. 7.** Nonmonotonic dependences of the induced loss and the resonance frequency shift of the probing wave on the pumping amplitude. The inset shows the result of numerical simulation of the mean compression of the Hertzian contact (first a decrease and then an increase) versus the increasing amplitude of the oscillating load.

#### *The Slow Dynamics of Dissipative and Elastic Properties with a Logarithmic Time Dependence*

The effects of the slow, logarithmic in time, dynamics are characterized by the remarkable similarity for a wide variety of materials with imperfect (defect) structures (a logarithmic creep, ageing, magnetic relaxation, etc.). Recently, a relaxation characterized by a logarithmic time dependence was observed in acoustically activated rock [21]. As a rule, such a behavior is ascribed to the complex relaxation dynamics of systems with a wide distribution of certain energy barriers characterizing the microstructural bonds in the material. The activation breaks these bonds, which later gradually recover under the effect of temperature fluctuations. The logarithmic-type relaxation is formed for a certain broad spectrum of these energy barriers, whose nature and relation to the microstructure of the material remain open to question [21]. Such a mechanism evidently implies a considerable asymmetry of the activation and relaxation processes (i.e., a fast breaking of bonds and a slow recovery). Note that, in addition to rocks with multiple defects [21], a slow relaxation and memory effects were observed for an ultrasound-activated single crack [22], for which the threshold of parametric generation of subharmonics and higher harmonics of the “reading wave” retained for several minutes a memory for the action of the other intense pumping wave.

In our experiments with samples containing single cracks, a slow drift of acoustic parameters was also observed. To reveal the features of these effects, the shape of the resonance peaks of the weak probing wave  $\varepsilon < 10^{-8}$  was recorded. Its behavior was studied for the first time both in the course of the activation of the sample by the pumping wave at another frequency (with

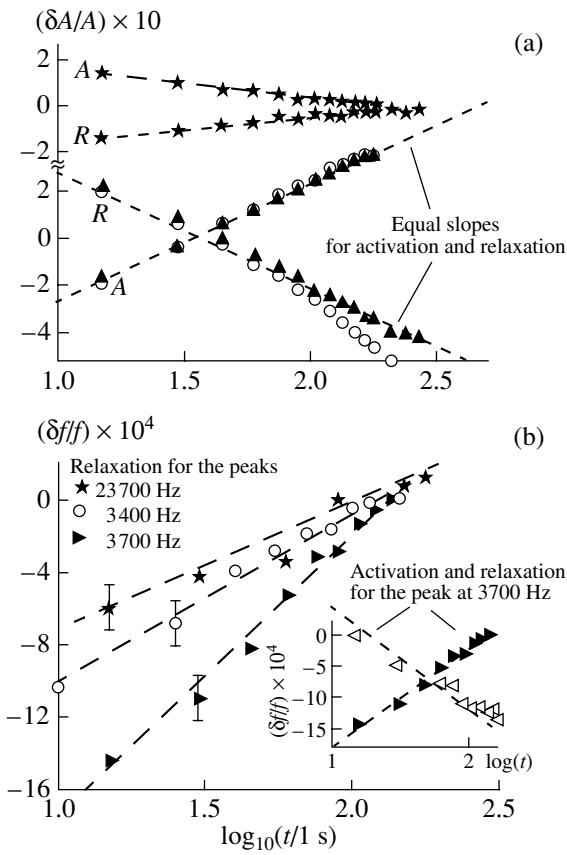


**Fig. 8.** Logarithmic dynamics of the probing wave in a glass rod with a crack. (a) Dynamics of the amplitude ( $Q$  factor) of the probing resonances with identical slopes of the dependences at the acoustic activation (indicated with A) and at the subsequent relaxation (indicated with R). (b) Analogous behavior of the resonance frequency shift at relaxation for several peaks and (inset) at both activation and relaxation for the peak at the frequency  $F = 3700$  Hz.

typical strains  $\varepsilon \sim 10^{-6} - 10^{-5}$ ) and after the pumping was switched off. The experiments revealed a slow dynamics for both dissipation (the  $Q$  factor of the probing resonance) and elastic properties (the position of the resonance peak). Figure 8 presents the corresponding dependences of the variations of the probing resonance maximum (proportional to the variations of the  $Q$  factor) and the shift of its position on the frequency axis,  $\delta f/f_0$ , as functions of the logarithm of the time interval, which was measured beginning from the instant of switching on or off the pumping wave. The logarithmic behavior of a single crack proved to be similar to the slow dynamics of the ensemble of numerous cracks in a rock sample [21]. However, an unexpected result was the symmetric reversibility of the logarithmic behavior; i.e., the slopes of the dependences obtained in the course of the activation and after its termination proved to be identical with a high accuracy. This does not agree with the hypothesis of breaking and recovery of some hypothetical bonds (inside the crack). At the same time,

in the context of the above discussion of the crack features, the reversible logarithmic behavior immediately follows from the locally cylindrical symmetry of heat flow propagation in the vicinity of the crack. Precisely the quasi-cylindrical geometry is characteristic of the areas of intense heat generation in the regions of stress concentration along the perimeter of the crack and at the line contacts, whose close-to-cylindrical character was independently determined from other considerations (see above). The deformation of the contacts under thermal stresses should lead to consequences similar to the “fast” effects governed by the action of elastic stresses on the contacts and should result in their displacements on the nanometer scale. From simple estimates, one can find that thermal strains can reach comparable values at the expense of temperature inhomogeneities on the order of  $\Delta T \sim 0.1 - 1$  K at the crack. Indeed, for a typical coefficient of thermal expansion  $\alpha \sim 3 \times 10^{-6} \text{ K}^{-1}$  and a typical crack size  $L \sim 3 \times 10^{-3}$  m, the resulting thermal displacement is  $\alpha L \Delta T \sim 10^{-9} - 10^{-8}$  m. Direct observations [23] of the surfaces of activated cracks by infrared cameras confirmed the possibility of their heating several degrees and higher. The logarithmically slow and time-reversible character of the local heating  $\Delta T$  of the center of the heat generation region in the two-dimensional (cylindrical) geometry immediately follows from the solution of the heat conduction equation  $\partial T/\partial t - D \Delta_{\perp} T = Q/(\rho C)$  with a cylindrical source  $Q(r, t)$  localized in a region of radius  $r \leq l$ . For heating, the asymptotically logarithmic solution has the form [18]

$$\Delta T \approx \frac{Q_F(k=0)}{4\pi\rho CD} \ln \frac{t}{l^2/D}, \text{ for } t \gg l^2/D = \omega_l^{-1}, \quad (7)$$

where  $k$  is the spatial harmonic of the Fourier transform  $Q_F(k)$  of the cylindrical source with respect to the radial coordinate. This solution is applicable to times up to  $t \leq l^2/D$ . Above this limit, the heat flow from the crack as a whole begins propagating as a heat flow from an object localized in three-dimensional space, and the local heating becomes saturated. For the subsequent cooling after switching off the source  $Q(r, t)$  at the instant  $t = t_0$  ( $t_0 \leq l^2/D$ ), we again arrive at an asymptotically logarithmic solution:

$$\Delta T \approx \frac{Q_F(k=0)}{4\pi\rho CD} \left[ \ln \frac{t_0}{l^2/D} - \ln \frac{(t-t_0)}{l^2/D} \right], \quad (8)$$

which is valid for  $l^2/D \ll t - t_0 \leq t_0$  and has the same coefficient multiplying the logarithmic factor as in Eq. (7). Thus, the observed symmetry of logarithmic activation and relaxation (Fig. 8) and the observed saturation of the logarithmic behavior at activation (within expected times on the order of hundreds of seconds for glass samples) are convincing arguments in favor of the pro-



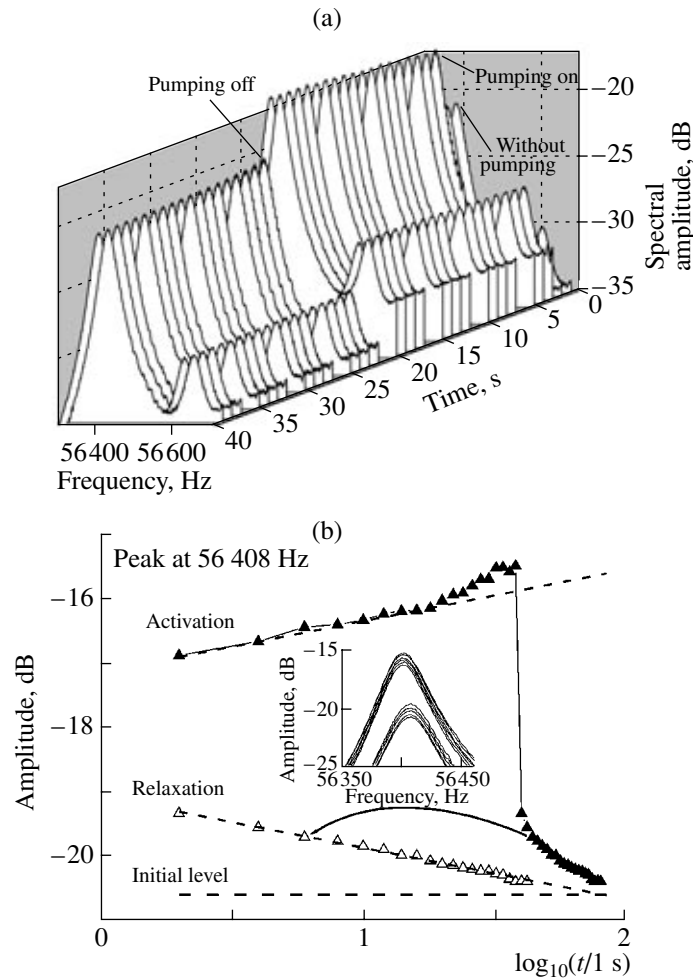


**Fig. 9.** Reversible logarithmic dynamics in the steel sample with a single crack. (a) A sequence of amplitude–frequency curves recorded for two neighboring resonances in the course of acoustic activation and the subsequent relaxation. (b) The amplitude of the peak at  $F = 56408$  Hz versus time in the course of activation by the pumping wave and the subsequent relaxation (full triangles; empty triangles show the dependence plotted anew for the relaxation process with the time measured starting from the instant of turning off the pumping). The inset shows the superimposed resonance curves demonstrating that the changes in absorption predominate over the changes in the resonance frequency, as in Figs. 3 and 7 for glass samples.

posed thermoelastic mechanism of the logarithmic slow dynamics.

The universality of this behavior was confirmed by the experiments with a bulk ( $36 \times 7 \times 6$  cm) steel sample containing a single crack about 1 cm in size. Figure 9 shows the symmetric and logarithmic-in-time dynamics observed for one of the resonances of the probing wave in this sample. Figure 9a displays a sequence of amplitude–frequency curves recorded for two neighboring resonances at a step of 1 s in the course of the acoustic activation of the sample by the pumping wave and the subsequent relaxation (after the pumping was turned off). Figure 9b shows the time dependences of the amplitude of one of the resonances ( $F = 56408$  Hz) with the time measurements starting from the instants of turning on and off the pumping wave for the respective curves. In Fig. 9, as in Fig. 8 for the glass sample, the symmetry of the activation and relaxation processes

is clearly pronounced. The characteristic times of the slow processes in Fig. 9 are smaller than those in Fig. 8, which agrees well with the proposed thermoelastic mechanism (in view of the difference in the thermal conductivities of glass and steel).

#### *Observation of a Memory in the Nonlinearity of a Crack*

The slow dynamics considered above is actually related to the variations of the linear acoustic properties of the sample with a crack (i.e., its resonance frequencies and  $Q$  factors). Attempts to detect slow effects in the nonlinear response (to compare our results with [22]) were hindered by the fact that the variations of nonlinearity-generated harmonics were determined to a considerable extent by variations of the sample resonance parameters, which masked the changes in the

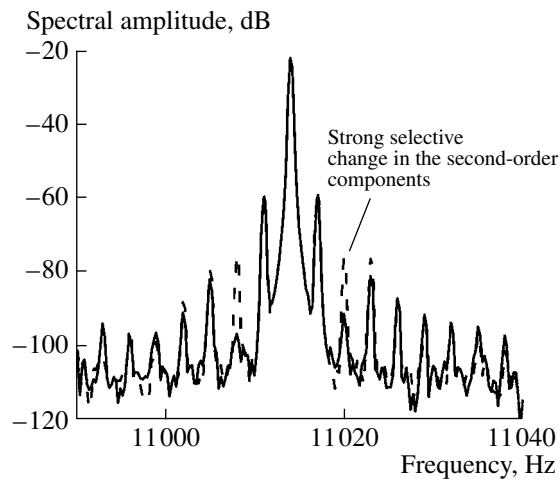


**Fig. 10.** Luxembourg–Gorki cross-modulation spectra of the probing wave for the sample that was preliminarily at rest (the dashed line) and for the same sample that was under the action of the pumping wave for several minutes (the solid line). The noticeable selective changes in the level of the second-order modulation components testify to the change in the character (parity) of the nonlinearity of the crack and to its memory for the activation.

nonlinearity of the crack. Using the Luxembourg–Gorki cross-modulation effect, for one of the glass resonators with a crack, we managed to demonstrate the memory associated with precisely the nonlinearity of the crack for the preceding acoustic activation. Figure 10 shows the cross-modulation spectra of the probing harmonic wave with frequency  $f_2 = 11015$  Hz that were obtained immediately after turning on the intense modulated pumping wave (with a carrier frequency  $f_2 \approx 3800$  Hz and a modulation frequency  $F = 2$  Hz) for the sample preliminarily being “at rest” and the spectra obtained for the same sample several minutes after the pumping was turned on. One can see a considerable difference between these spectra in the level of the second modulation component (more than 15 dB), which testifies to a significant change in the character (parity) of nonlinearity. At the same time, the amplitude variations of the fundamental harmonic and other components were insignificant: this suggests that the linear characteristics of the given resonance varied only slightly and, therefore, could not selectively affect the second-order components.

The possibility of a change in the character (parity) of nonlinearity agrees well with the aforementioned nonmonotonicity of the dependence of the average contact width on the pumping amplitude (see the inset in Fig. 7). As long as the amplitude of the modulated (with frequency  $F$ ) pumping does not pass through the minimum of this dependence, the modulation of the average contact width mainly contains the  $F$  harmonic. After passing through the minimum, the induced increase in the contact width occurs twice within the modulation

period, which leads to a sharp growth of the  $2F$  harmonic in the contact modulation. Such a passage of the “operating point” through the minimum may be caused by a change in the pumping amplitude itself or a change in the initial contact compression due to thermoelastic effects at constant pumping amplitude.

## CONCLUSIONS

In the series of experiments with glass and steel samples with cracks, we studied such effects as the time-reversible slow logarithmic dynamics of the elastic and inelastic properties of acoustically activated single cracks, as well as a number of important features of “fast” nonlinear effects: the modulation spectrum transfer of the Luxembourg–Gorki type due to the interaction of acoustic waves at the cracks and the slow dynamics of this effect; the nonmonotonic amplitude behavior and the manifestation of the crack state changes of opposite character for different frequencies of the probing wave (i.e., the simultaneous observation of the induced clarification for some probing modes and absorption for other probing modes). The mechanism of acoustic wave interaction with cracks that was proposed to explain the experimental results is at variance with the commonly accepted idea that the role of thermoelastic effects is insignificant, including the case of the linear (small-amplitude) absorption of elastic waves in rock. The results obtained above give an insight into the physics of both fast and slow wave processes in cracked media. The observed nonlinear acoustic effects, which exhibit a high sensitivity to the presence of cracks in solids, offer considerable promise for the development of new nonlinear-modulation methods for detecting cracks and cracklike defects.

## ACKNOWLEDGMENTS

This work was supported in part by the Russian Foundation for Basic Research (project no. 05-02-17355), the Ministry of Industry and Science (NSh-1641.2003.2), and the Russian Science Support Foundation (V.Z.). The experiments were performed at the Laboratory of Acoustics of Université du Maine (France) under the PAI–Russie and PECO–NEI Programs (project nos. 04521TM and 16366).

## REFERENCES

1. G. M. Mavko and A. Nur, *J. Geophys. Res.* **83** (B9), 4459 (1978).
2. G. M. Mavko and D. Jizba, *Geophysics* **59** (1), 87 (1994).
3. V. E. Nazarov, A. V. Radostin, and I. A. Soustova, *Akust. Zh.* **48**, 85 (2002) [*Acoust. Phys.* **48**, 76 (2002)].
4. R. B. Gordon and L. A. Davis, *J. Geophys. Res.* **73** (12), 3917 (1968).

5. R. R. Stewart and M. N. Toksoz, *J. Geophys. Res.* **88** (B1), 546 (1983).
6. R. W. Carpick, Q. Dai, D. F. Ogletree, and M. Salmeron, *Tribol. Lett.* **5**, 91 (1998).
7. J. S. Savage, *J. Geophys. Res.* **71** (16), 3929 (1966).
8. V. Zaitsev, V. Gusev, and B. Castagnede, *Phys. Rev. Lett.* **89** (10), 105502 (2002).
9. G. Mavko, *J. Geophys. Res.* **84** (B9), 4769 (1979).
10. V. Zaitsev and P. Sas, *Acust. Acta Acust.* **86**, 429 (2000).
11. L. D. Landau and E. M. Lifshitz, *Theory of Elasticity* (Nauka, Moscow, 1965; Pergamon, Oxford, 1986).
12. D. Broek, *Elementary Engineering Fracture Mechanics* (Noordhoff, Leyden, 1974; Vysshaya Shkola, Moscow, 1980).
13. E. J. Johnson, *Contact Mechanics* (Cambridge Univ. Press, Cambridge, 1987; Mir, Moscow, 1989).
14. B. D. H. Tellegen, *Nature*, No. 6, 840 (1933).
15. V. L. Ginzburg, *Izv. Akad. Nauk SSSR*, No. 12, 253 (1948).
16. A. L. Bagmet, V. E. Nazarov, A. V. Nikolaev, *et al.*, *Dokl. Akad. Nauk* **346** (3), 390 (1996).
17. V. Zaitsev, V. Gusev, and B. Castagnede, *Ultrasonics* **40**, 627 (2002).
18. V. Zaitsev, V. Gusev, and B. Castagnede, *Phys. Rev. Lett.* **90** (7), 075501 (2003).
19. I. Solodov, *Ultrasonics* **36**, 383 (1998).
20. O. Kolosov and K. Yamanaka, *Jpn. J. Appl. Phys.* **32**, L1095 (1993).
21. J. A. Ten Cate, E. Smith, and R. A. Guyer, *Phys. Rev. Lett.* **85** (5), 1020 (2000).
22. I. Solodov and B. Korshak, *Phys. Rev. Lett.* **88** (1–4), 014303 (2002).
23. L. D. Favro, Xiaoyan Han, Zhong Ouyang, *et al.*, *Rev. Sci. Instrum.* **71** (6), 2418 (2000).

*Translated by E. Golyamina*